Measurement and Modelling of Interference Alignment Impairments

Martin Mayer, Maxime Guillaud, Gerald Artner and Markus Rupp

Institute of Telecommunications, Vienna University of Technology

Gusshausstrasse 25/E389, A-1040 Vienna, Austria

Email: mmayer@nt.tuwien.ac.at, guillaud@tuwien.ac.at, gartner@nt.tuwien.ac.at, mrupp@nt.tuwien.ac.at.

Abstract—Interference alignment is a linear precoding technique that eliminates interference in the K-user interference channel. We present measurement results and identify the performance limiting factors that occur under real conditions. In our setup, we found the main causes of impairment to be outdated channel state information in varying channels, thermal noise at the receiver and transmit impairments. We propose a simplistic channel model that is capable of capturing these effects and allows to investigate their impact on the achievable rate.

I. INTRODUCTION

Interference Alignment (IA) was proposed in [1] to approach the maximum degrees of freedom in the K-user interference channel. In this work, we consider spatial IA [2] enabled by Multiple-Input Multiple-Output (MIMO) transmissions. With global channel knowledge, precoders can be computed [3] in such a way that the interfering signals are aligned in an interference subspace at each receiver. As the interference subspace and the desired signal subspace are generally linearly independent, interference can be cancelled by applying a suitable receive filter.

In practical systems, the performance of IA faces several limitations. Transmit impairments as investigated in [4]–[6] induce noisy transmit signals, thermal noise is present at the receiver and the channels exhibit fluctuations. All these effects accumulate to imperfect channel knowledge [7] which strongly hampers the performance.

While the general impact of spurious effects on IA has been studied in literature such as [8], [9], to the best of the author's knowledge there exists no particular description of how the individual effects amount to misaligned interference in a real setup.

In our previous work [10], we investigated the performance of IA with online precoder computation and feedback with the Vienna MIMO Testbed (VMTB). The same setup is now used to measure the rate versus variable Signal to Noise Ratio (SNR) at a constant Signal to Interference Ratio (SIR) of $-3\,\mathrm{dB}$. We investigate the individual spurious effects that lead to suboptimal alignment based on the interference leakage power. A simplistic channel model helps us to understand to what extent the channel fluctuations, receive noise and transmit impairments amount to the interference leakage power.

The remainder of this paper is organized as follows. Section II describes our version of the K-user interference channel and the basics of IA. In Section III, the VMTB setup and measurement methodology is recapitulated and a suitable channel model is deduced from measurements. Section IV discusses the derivation of the performance impairing terms by means of mutual information and interference leakage power. Section V illustrates the findings by comparing the data rate of perfect and real IA in the measured and simulated case. Section VI concludes the paper.

Notation: $\mathbb{E}[\cdot]$ denotes the expectation operator, $\mathrm{Tr}[\cdot]$ is the trace of a matrix, $\mathrm{vec}[\cdot]$ arranges the columns of a matrix in a vector and the superscript $^{\mathrm{H}}$ denotes the conjugate transpose. The abbreviation i.i.d. stands for independent and identically distributed.
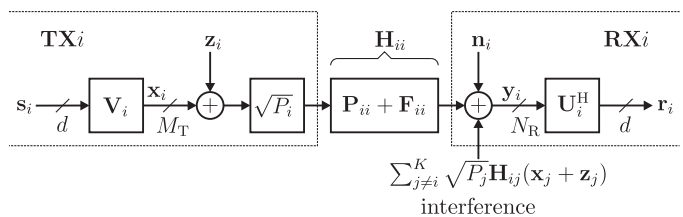

Fig. 1. Channel model for the ith user of the interference channel.

II. INTERFERENCE ALIGNMENT IN THE K-USER MIMO INTERFERENCE CHANNEL

We consider the symmetric case of the K-user MIMO interference channel, where a link – depicted in Figure 1 – comprises M_{T} transmit antennas and N_{R} receive antennas. At transmitter $j \in \{1, ..., K\}$, a data stream $\mathbf{s}_j \in \mathbb{C}^d$ with $\mathbb{E}[\mathbf{s}_j\mathbf{s}_j^{\mathrm{H}}] = \mathbf{I}_d$ is filtered by a linear precoder $\mathbf{V}_j \in \mathbb{C}^{M_{\mathrm{T}} \times d}$ to obtain the transmit vector $\mathbf{x}_j \in \mathbb{C}^{M_{\mathrm{T}}}$. A transmit noise term $\mathbf{z}_j \in \mathbb{C}^{M_{\mathrm{T}}}$ is added, accounting for transmit impairments and modeled as additive white Gaussian noise as proposed in [4] with zero mean and covariance $\sigma_{z_j}^2 \mathbf{I}_{M_{\mathrm{T}}}$. The transmit vector is scaled by $\sqrt{P_j}$ to normalize the transmit signal power to $\mathrm{Tr}[\mathbb{E}[\mathbf{x}_j\mathbf{x}_j^{\mathrm{H}}]] = P_j d$. Channel matrix $\mathbf{H}_{ij} \in \mathbb{C}^{N_{\mathrm{R}} \times M_{\mathrm{T}}}$ represents the channel coefficients for the MIMO transmission between transmitter j and receiver $i \in \{1, ..., K\}$. At receiver i, a noise vector $\mathbf{n}_i \in \mathbb{C}^{N_{\mathrm{R}}}$ is added, it accounts for thermal noise and is modeled as additive white Gaussian noise with zero mean and covariance $\sigma_{n_i}^2 \mathbf{I}_{N_{\mathrm{R}}}$. Receive vector $\mathbf{y}_i \in \mathbb{C}^{N_{\mathrm{R}}}$ is filtered by a receive filter $\mathbf{U}_i \in \mathbb{C}^{N_{\mathrm{R}} \times d}$ and receive data stream $\mathbf{r}_i \in \mathbb{C}^d$ reads

$$\mathbf{r}_i = \underbrace{\sqrt{P_i}\mathbf{U}_i^{\mathrm{H}}\mathbf{H}_{ii}\mathbf{V}_i\mathbf{s}_i}_{\text{desired signal}} + \underbrace{\sum_{\substack{j=1 \\ j \neq i}}^{K} \sqrt{P_j}\mathbf{U}_i^{\mathrm{H}}\mathbf{H}_{ij}\mathbf{V}_j\mathbf{s}_j}_{\text{interference}} + \underbrace{\mathbf{U}_i^{\mathrm{H}}(\mathbf{n}_i + \widetilde{\mathbf{z}}_i)}_{\text{noise}},$$

$$\text{(1)}$$

where $\widetilde{\mathbf{z}}_i \in \mathbb{C}^{N_{\mathrm{R}}}$ is the filtered transmit noise

$$\widetilde{\mathbf{z}}_i = \sum_{j=1}^{K} \sqrt{P_j}\mathbf{H}_{ij}\mathbf{z}_j. \qquad (2)$$

Note that for a fixed deterministic channel realization $\mathbf{H}_{ij}$, $\widetilde{\mathbf{z}}_i$ is spatially colored in general with covariance $\mathbf{Q}_{\widetilde{z}_i}$.

Relying on global channel knowledge, the precoders and receive filters for IA are jointly computed to satisfy

$$\mathbf{U}_i^{\mathrm{H}}\mathbf{H}_{ij}\mathbf{V}_j = \mathbf{0}, \forall j \neq i, \qquad (3a)$$

$$\mathrm{rank}(\mathbf{U}_i^{\mathrm{H}}\mathbf{H}_{ii}\mathbf{V}_i) = d, \forall i \in \{1, ..., K\}. \qquad (3b)$$

(3a) describes the interference cancellation, and (3b) states that the effective MIMO channel of a desired link retains full rank $d < \min(M_{\mathrm{T}}, N_{\mathrm{R}})$. The rank reduction compared to the full MIMO multiplexing gain is a result of partitioning the receive signal space into a desired signal subspace of dimension d and an interference subspace of dimension $N_{\mathrm{R}} - d$.
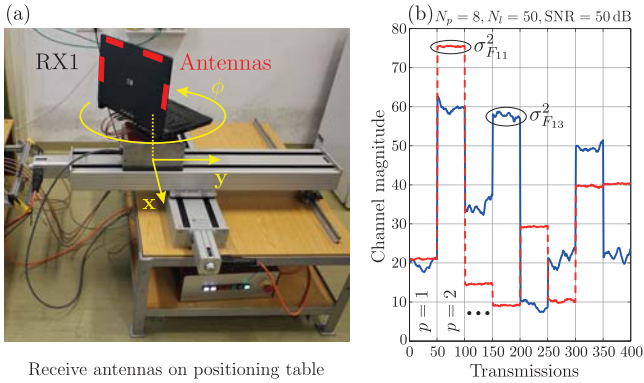
Fig. 2. (a) Receiver RX1 located on 5th floor of the Institute of Telecommunications at Vienna University of Technology. (b) Example of the estimated outdoor to indoor channel $|\widehat{\mathbf{H}}_{11}|$ (blue solid line) and indoor to indoor channel $|\widehat{\mathbf{H}}_{13}|$ (red dashed line) computed from each received frame.

III. MEASUREMENT SETUP AND MODEL DEDUCTION

The VMTB in the considered setup is composed of two outdoor (rooftop) transmitters TX1 and TX2 equipped with a Kathrein 800 10543 XX-pol outdoor antenna, one indoor transmitter TX3 equipped with two 800 10677 X-pol indoor antennas and one indoor receiver RX1 with four custom built $\lambda/2$ dipoles incorporated in a laptop chassis that is mounted on an x–y–ϕ positioning table depicted in Figure 2 (a). We thus obtain $M_T = N_R = 4$, $K = 3$ and chose $d = 2$. The testbed operates at a commerical carrier frequency of 2.503 GHz. In order to keep computation times low, we only use a single subcarrier of an Orthogonal Frequency Division Multiplexing (OFDM) transmission. RX1 performs the filter computation and feeds the precoders back to TX1-3 via a dedicated fiber network. Please refer to [10] for more details on our setup.

We intend to average our results (powers and rate) over various receiver positions (space) and time and to investigate the influence of spatial and temporal channel change. To that end, N_l frames indexed by l are transmitted at fixed position, the receive antennas are moved into a new position indexed by p and again N_l frames are transmitted. This is repeated for N_p positions. The measures computed from each frame are hence indexed by the superscript $^{(p,l)}$.

In order to describe the channel changes over space and time, we model the channel matrix as the sum of a position dependent matrix $\mathbf{P}_{ij}^{(p)} \in \mathbb{C}^{N_R \times M_T}$ and an independent time variant matrix $\mathbf{F}_{ij}^{(l)} \in \mathbb{C}^{N_R \times M_T}$:

$$\mathbf{H}_{ij}^{(p,l)} = \mathbf{P}_{ij}^{(p)} + \mathbf{F}_{ij}^{(l)}. \tag{4}$$

In Figure 2 (b), the magnitude of two estimated channel coefficients is plotted over $N_l \times N_p = 400$ channel realizations. One is an entry of $|\widehat{\mathbf{H}}_{11}|$ (outdoor to indoor channel), the other one is an entry of $|\widehat{\mathbf{H}}_{13}|$ (indoor to indoor channel). We observe a strong position dependency which is evoked by small scale fading that can be modeled with a Rayleigh distribution in good approximation. At each new position p, the entries of $\mathbf{P}_{ij}^{(p)}$ are therefore drawn independently (no antenna correlation) from a circularly symmetric complex normal distribution with zero mean and variance $\sigma_{P_{ij}}^2$. At fixed position, we observe that the channels change between transmissions and that these fluctuations are stronger on the outdoor to indoor channel. We model this behavior by independently drawing the entries of $\mathbf{F}_{ij}^{(l)}$ from a circularly symmetric complex normal distribution with zero mean and variance $\sigma_{F_{ij}}^2$ that determines the strength of the channel change over time. Considering that a frame is about 8 ms long and that the computation time between successive frames takes about 70 ms, we assume block fading, i.e., the channel stays constant during one frame but changes between frames.

Each frame is a concatenation of a zero vector, a pilot preamble and a data payload. The zero vector is received as $\mathbf{r}_{i,\text{noise}}^{(p,l)} = \mathbf{U}_i^{(p,l)\text{H}} \left(\mathbf{n}_i^{(p,l)} + \widetilde{\mathbf{z}}_i^{(p,l)} \right)$ and is used to estimate the noise covariance matrix (utilizing all frames)

$$\widehat{\mathbf{Q}}_{\text{N},i} = \frac{1}{N_p N_l} \sum_{p=1}^{N_p} \sum_{l=1}^{N_l} \mathbf{r}_{i,\text{noise}}^{(p,l)} \mathbf{r}_{i,\text{noise}}^{(p,l)\text{H}}. \tag{5}$$

Note that receive noise covariance $\sigma_{n_i}^2 \mathbf{I}_d$ without transmit noise can be estimated by turning off all transmitters. The pilot preamble contains training sequences of length N_{PS} that are optimal for least squares channel estimation as proposed in [11]. The so obtained transmit power scaled channel estimates read

$$\widehat{\mathbf{H}}_{ij}^{(p,l)} = \sqrt{P_j}\mathbf{H}_{ij}^{(p,l)} + \mathbf{N}_i^{(p,l)}, \tag{6}$$

where $\mathbf{N}_i^{(p,l)} \in \mathbb{C}^{N_R \times M_T}$ is the channel estimation noise matrix. In order to estimate position variance $\sigma_{P_{ij}}^2$ from the measurements, we first compute the position dependent mean of the channel estimates

$$\overline{\mathbf{H}}_{ij}^{(p)} = \frac{1}{N_l} \sum_{l=1}^{N_l} \widehat{\mathbf{H}}_{ij}^{(p,l)} \tag{7}$$

that stores the realizations of $\mathbf{P}_{ij}^{(p)}$ over $p = 1...N_p$. It is then used to estimate the position variance

$$\hat{\sigma}_{P_{ij}}^2 = \alpha \frac{1}{N_p} \sum_{p=1}^{N_p} \text{Tr}\left[\text{vec}\left[\overline{\mathbf{H}}_{ij}^{(p)} \right] \text{vec}\left[\overline{\mathbf{H}}_{ij}^{(p)} \right]^\text{H} \right], \tag{8}$$

where $\alpha = \frac{1}{P_j}\frac{1}{M_T N_R}$. Due to temporal correlations in the measured channels – visible in Figure 2 (b) – that are not part of the model, a similar direct approach as in (8) is not suitable to accurately estimate the temporal fluctuations quantified by $\sigma_{F_{ij}}^2$. Instead, we found (9) to be appropriate:

$$\hat{\sigma}_{F_{ij}}^2 = c\alpha \frac{1}{N_p N_l - 1} \sum_{p=1}^{N_p} \sum_{l=1}^{N_l} \text{Tr}\left[\text{vec}\left[\breve{\mathbf{H}}_{ij}^{(p,l)} \right] \text{vec}\left[\breve{\mathbf{H}}_{ij}^{(p,l)} \right]^\text{T} \right], \tag{9}$$

with $\breve{\mathbf{H}}_{ij}^{(p,l)} = \left| \widehat{\mathbf{H}}_{ij}^{(p,l)} - \overline{\mathbf{H}}_{ij}^{(p)} \right|$ and a scaling factor c chosen to optimally fit the measurements; the underlying curve fit is described in Section V. Note that the estimation of $\sigma_{P_{ij}}^2$ and $\sigma_{F_{ij}}^2$ requires high SNR, i.e., the additive noise can be neglected.

IV. IMPACT ON INTERFERENCE ALIGNMENT

At each position p and frame l, channels are estimated and receive filters $\mathbf{U}_i^{(p,l)}$ and precoders $\mathbf{V}_j^{(p,l)}$ that satisfy (3a) are computed therewith. The precoders are then distributed among the transmitters and applied on the data streams of frame $l + 1$. Because the channel estimates at frame $l + 1$ contain different noise and channel realizations, the filters that were computed at frame l do not satisfy (3a) perfectly anymore. This results in interference leakage, i.e., power from the interferers leaks into the desired signal subspace at the receiver and can no longer be canceled.

Our measurements took place in a vacant laboratory room which yields quasi-static channels that exhibit only small changes over time. In comparison, receiver repositioning and the inherent small scale fading causes strong channel variations — measurements at an average SNR of 50 dB and SIR of −3 dB showed that moving the receiver by 10% of the wavelength caused the data rate to drop by more than one half if we apply the outdated filters from the previous position. In the following, we focus on the impact of the temporal fluctuation, receiver repositioning is only used to ensure proper averaging over small scale fading. We therefore exclude the first frame after each receiver repositioning in the mutual information

and interference leakage power computation by omitting index p; the channel changes are then due to temporal fluctuation only.

Mutual information as a measure for achievable data rate is now introduced. Using (1) and the property $\mathbf{U}_i^{\mathrm{H}}\mathbf{U}_i = \mathbf{I}_d$, the receive data covariance computed from frame $l+1$ is given by[1]

$$
\begin{aligned}
\mathbf{Q}_{\mathbf{r}_i}^{(l+1)} &= \mathbb{E}_{\mathbf{r}}\left[\mathbf{r}_i\mathbf{r}_i^{\mathrm{H}}\right] \\
&= \underbrace{P_i\mathbf{U}_i^{(l)\mathrm{H}}\mathbf{H}_{ii}^{(l+1)}\mathbf{V}_i^{(l)}(\mathbf{U}_i^{(l)\mathrm{H}}\mathbf{H}_{ii}^{(l+1)}\mathbf{V}_i^{(l)})^{\mathrm{H}}}_{\mathbf{Q}_{\mathrm{S},i}^{(l+1)}} + \\
&\quad \underbrace{\sum_{\substack{j=1\\j\neq i}}^{K} P_j\mathbf{U}_i^{(l)\mathrm{H}}\mathbf{H}_{ij}^{(l+1)}\mathbf{V}_j^{(l)}(\mathbf{U}_i^{(l)\mathrm{H}}\mathbf{H}_{ij}^{(l+1)}\mathbf{V}_j^{(l)})^{\mathrm{H}}}_{\mathbf{Q}_{\mathrm{I},i}^{(l+1)}} + \\
&\quad \underbrace{\sigma_{n_i}^2\mathbf{I}_d + \mathbf{U}_i^{(l)\mathrm{H}}\mathbf{Q}_{\widetilde{\mathbf{z}}_i}\mathbf{U}_i^{(l)}}_{\mathbf{Q}_{\mathrm{N},i}^{(l+1)}},
\end{aligned}
\tag{10}
$$

where $\mathbf{Q}_{\mathrm{S},i}$, $\mathbf{Q}_{\mathrm{I},i}$ and $\mathbf{Q}_{\mathrm{N},i}$ are the respective covariance matrices of the signal of interest, interference leakage and noise at receiver i after interference suppression with the receive filter $\mathbf{U}_i$. The mutual information between transmit data stream $\mathbf{s}_i$ and receive data stream $\mathbf{r}_i$ of frame l is then defined according to [12] as

$$
\mathcal{I}(\mathbf{s}_i;\mathbf{r}_i)^{(l)} = \log_2\det\left[\mathbf{I}_d + \mathbf{Q}_{\mathrm{S},i}^{(l)}\left(\mathbf{Q}_{\mathrm{I},i}^{(l)} + \mathbf{Q}_{\mathrm{N},i}^{(l)}\right)^{-1}\right].
\tag{11}
$$

A growth in $\mathbf{Q}_{\mathrm{I},i}$ or $\mathbf{Q}_{\mathrm{N},i}$ reduces mutual information. In the following, we are particularly interested in how the model parameters influence the interference leakage covariance $\mathbf{Q}_{\mathrm{I},i}$. Therefore, we apply (3a), (4), (6) and the substitution $\widetilde{\mathbf{F}}_{ij} = \mathbf{F}_{ij}^{(l+1)} - \mathbf{F}_{ij}^{(l)}$ on the highlighted (red) term in (10)

$$
\begin{aligned}
&\mathbf{U}_i^{(l)\mathrm{H}}\mathbf{H}_{ij}^{(l+1)}\mathbf{V}_j^{(l)} = \mathbf{U}_i^{(l)\mathrm{H}}\frac{1}{\sqrt{P_j}}\left(\widehat{\mathbf{H}}_{ij}^{(l+1)} - \mathbf{N}_i^{(l+1)}\right)\mathbf{V}_j^{(l)} = \\
&\underbrace{\mathbf{U}_i^{(l)\mathrm{H}}\widetilde{\mathbf{F}}_{ij}\mathbf{V}_j^{(l)}}_{\text{fluctuation}} - \frac{1}{\sqrt{P_j}}\underbrace{\mathbf{U}_i^{(l)\mathrm{H}}\mathbf{N}_i^{(l)}\mathbf{V}_j^{(l)}}_{\text{chan. est. noise}} + \frac{1}{\sqrt{P_j}}\underbrace{\mathbf{U}_i^{(l)\mathrm{H}}\widehat{\mathbf{H}}_{ij}^{(l)}\mathbf{V}_j^{(l)}}_{=\mathbf{0}\ \forall j\neq i}
\end{aligned}
\tag{12}
$$

and thus obtain a term that depends on the channel fluctuations between transmissions $\widetilde{\mathbf{F}}_{ij}$ and a term that depends on channel estimation noise $\mathbf{N}_i^{(l)}$ — if the channels stay perfectly constant and there is no noise, interference leakage is zero. We now consider the average over many channel realizations (frames) l. Doing so, the received transmit noise $\widetilde{\mathbf{z}}_i$ from (2) becomes spatially white in expectation, i.e., $\mathbb{E}_{\mathbf{H},\mathbf{z}}\left[\widetilde{\mathbf{z}}_i\widetilde{\mathbf{z}}_i^{\mathrm{H}}\right] = \mathbf{Q}_{\widetilde{\mathbf{z}}_i} = \sigma_{\widetilde{z}_i}^2\mathbf{I}_{N_R}$ with $\sigma_{\widetilde{z}_i}^2 = \sum_{j=1}^{K} M_{\mathrm{T}}P_j(\sigma_{P_{ij}}^2 + \sigma_{F_{ij}}^2)\sigma_{z_j}^2$, since $\mathbf{H}_{ij}$ and $\mathbf{z}_j$ have i.i.d. entries, respectively. Furthermore, the entries of the channel estimation noise matrix $\mathbf{N}_i$ that appears in (6) have variance $\frac{1}{N_{\mathrm{PS}}}(\sigma_{n_i}^2 + \sigma_{\widetilde{z}_i}^2)$. An increasing pilot sequence length N_{PS} thus decreases the channel estimation noise variance.

The average interference leakage power at RXi is now obtained by plugging the result from (12) back into $\mathbf{Q}_{\mathrm{I},i}$ of (10) and compute[2]

$$
P_{\mathbf{Q}_{\mathrm{I},i}} = \mathbb{E}_{\mathbf{H},\mathbf{N}}\left[\mathrm{Tr}\left[\mathbf{Q}_{\mathrm{I},i}\right]\right] = P_{\widetilde{\mathbf{F}}_i} + P_{\mathbf{n}_i} + P_{\widetilde{\mathbf{z}}_i}
\tag{13}
$$

which comprises the average interference leakage power caused by temporal fluctuation

$$
P_{\widetilde{\mathbf{F}}_i} = 2d^2\sum_{\substack{j=1\\j\neq i}}^{K} P_j\sigma_{F_{ij}}^2,
\tag{14}
$$

the average interference leakage power caused by channel estimation receive noise

$$
P_{\mathbf{n}_i} = \frac{d^2(K-1)}{N_{\mathrm{PS}}}\sigma_{n_i}^2,
\tag{15}
$$

and the average interference leakage power caused by channel estimation transmit noise

$$
P_{\widetilde{\mathbf{z}}_i} = \frac{d^2(K-1)}{N_{\mathrm{PS}}}\sum_{j=1}^{K} M_{\mathrm{T}}P_j(\sigma_{P_{ij}}^2 + \sigma_{F_{ij}}^2)\sigma_{z_j}^2.
\tag{16}
$$

Similarly, the noise power at the receiver is

$$
P_{\mathbf{Q}_{\mathrm{N},i}} = \mathbb{E}_{\mathbf{N}}[\mathrm{Tr}[\mathbf{Q}_{\mathrm{N},i}]] = d\left(\sigma_{n_i}^2 + \sum_{j=1}^{K} M_{\mathrm{T}}P_j(\sigma_{P_{ij}}^2 + \sigma_{F_{ij}}^2)\sigma_{z_j}^2\right).
\tag{17}
$$

These terms are used to make qualitative statements on how channel fluctuations and noise reduce or limit mutual information.

V. Results and Discussion

Our testbed employs programmable attenuators at the radio-frequency frontend of each transmitter which allow to vary the transmit powers individually. The average receive SIR over the N_p positions shall be $-3\,\mathrm{dB}$, i.e., the three transmitters are received equally strong at receiver of choice i. Note that this implies that the interference power at this receiver is on average twice as strong as the desired signal power. This is accomplished by randomly picking N_p positions prior to the measurement, measuring the average transmit power contribution from transmitter j to receiver i over these specific positions utilizing the channel estimates from (6)

$$
P_{ij} = \frac{1}{N_pN_l}\sum_{p=1}^{N_p}\sum_{l=1}^{N_l}\mathrm{Tr}\left[\mathrm{vec}\left[\widehat{\mathbf{H}}_{ij}^{(p,l)}\right]\mathrm{vec}\left[\widehat{\mathbf{H}}_{ij}^{(p,l)}\right]^{\mathrm{H}}\right] - \frac{P_{\mathbf{Q}_{\mathrm{N},i}}}{N_{\mathrm{PS}}},
\tag{18}
$$

and then adjusting the transmit powers P_j to achieve equal P_{ij} ($\forall j$) at receiver of choice i. All subsequent measurements take place at these specific positions. The receive SNR is computed as $10\log_{10}\frac{P_{ii}}{d\sigma_{n_i}^2}$ dB, the received transmit noise $\widetilde{\mathbf{z}}_i$ is regarded as a spurious effect and is not considered in the SNR. To vary the receive SNR at constant SIR, the transmit powers are correspondingly altered (adding $3\,\mathrm{dB}$ to all P_j increases SNR by $3\,\mathrm{dB}$). The covariance matrices in (10) are approximated with channel estimates from (6)

$$
\widehat{\mathbf{Q}}_{\mathrm{S},i}^{(l+1)} = \mathbf{U}_i^{(l)\mathrm{H}}\widehat{\mathbf{H}}_{ii}^{(l+1)}\mathbf{V}_i^{(l)}(\mathbf{U}_i^{(l)\mathrm{H}}\widehat{\mathbf{H}}_{ii}^{(l+1)}\mathbf{V}_i^{(l)})^{\mathrm{H}},
\tag{19a}
$$

$$
\widehat{\mathbf{Q}}_{\mathrm{I},i}^{(l+1)} = \sum_{\substack{j=1\\j\neq i}}^{K}\mathbf{U}_i^{(l)\mathrm{H}}\widehat{\mathbf{H}}_{ij}^{(l+1)}\mathbf{V}_j^{(l)}(\mathbf{U}_i^{(l)\mathrm{H}}\widehat{\mathbf{H}}_{ij}^{(l+1)}\mathbf{V}_j^{(l)})^{\mathrm{H}}
\tag{19b}
$$

and the approximated mutual information of frame l reads

$$
\widehat{\mathcal{I}}(\mathbf{s}_i;\mathbf{r}_i)^{(l)} = \log_2\det\left[\mathbf{I}_d + \widehat{\mathbf{Q}}_{\mathrm{S},i}^{(l)}\left(\widehat{\mathbf{Q}}_{\mathrm{I},i}^{(l)} + \widehat{\mathbf{Q}}_{\mathrm{N},i}^{(l)}\right)^{-1}\right].
\tag{20}
$$

Note that the channel estimates bear an additional noise term; calculations have shown that this term doubles the interference leakage power in (15) and (16). The ramifications and bounds of mutual information approximation with channel estimates are discussed in [7].

Figure 3 depicts the interference leakage power over SNR in various cases. It is influenced by $P_{\mathbf{n}_1}$ that is constant over SNR and by $P_{\widetilde{\mathbf{z}}_1}$ and $P_{\widetilde{\mathbf{F}}_1}$ that both exhibit a direct transmit power dependency. The strength of temporal channel fluctuation is controlled by $\sigma_{F_{ij}}^2$, it determines at which SNR $P_{\widetilde{\mathbf{F}}_1}$ grows larger than $P_{\mathbf{n}_1}$. Factor c in (9) is chosen such that the measured curve overlaps with the simulation. The analytic curve is obtained by computing (13) with the estimated parameters and plotting $10\log_{10}P_{\mathbf{Q}_{\mathrm{I},1}}$.
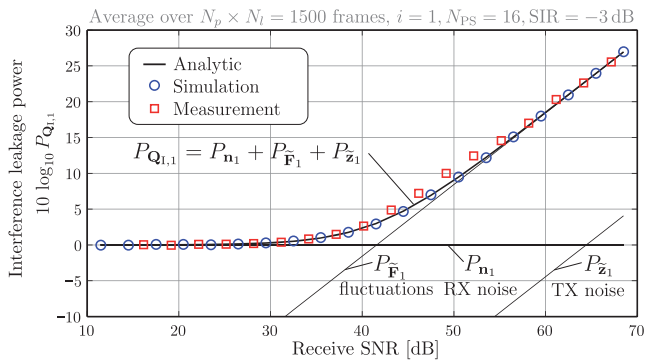
---

[1]Index p is omitted and the expectation $\mathbb{E}_{\mathbf{r}}[\cdot]$ is with respect to all received data vectors $\mathbf{r}$ of frame $l+1$.

[2]Note that the expectation with respect to $\mathbf{H}$ and $\mathbf{N}$ entails the random matrices $\mathbf{F}$, $\mathbf{P}$ and the random vectors $\mathbf{n}$, $\mathbf{z}$.

Fig. 3.   Interference leakage power $P_{\mathbf{Q}_{I,1}}$ vs. SNR.

Fig. 4.   Mutual information approximation $\widehat{\mathcal{I}}(\mathbf{s}_1; \mathbf{r}_1)$ vs. SNR.

Figure 4 shows the approximated mutual information $\widehat{\mathcal{I}}(\mathbf{s}_1; \mathbf{r}_1)$ that is averaged over all $N_p \times N_l = 30 \times 50 = 1500$ transmissions. Perfect IA denotes the case where interference leakage is zero, i.e., $\mathbf{Q}_{I,1} = \mathbf{0}$ (and thus $P_{\mathbf{Q}_{I,1}} = 0$), and real IA is the truly achieved leakage-impaired version. For comparison, a synthetic Time Division Multiple Access (TDMA)[3] curve is also plotted. It achieves $\frac{1}{K} = \frac{1}{3}$ of the interference-free rate, whereas IA ideally achieves $\frac{1}{2}$ of it.

At low SNR, the leakage power due to channel estimation receive noise $P_{\mathbf{n}_1}$ is dominant, which causes a gap between the mutual information of the perfect IA case and the real IA case due to the additional noise term $P_{\mathbf{n}_1}$ in $P_{\mathbf{Q}_{I,1}}$. Increasing the SNR also increases the interference power (since $\text{SIR} = -3\,\text{dB}$) and at some point, the leakage power due to temporal fluctuation $P_{\widetilde{\mathbf{F}}_1}$ grows larger than the noise and becomes dominant. This ultimately causes the mutual information to saturate at high SNR, because the interference powers P_j ($j \neq 1$) in $\mathbf{Q}_{I,1}$ are proportional to the desired signal power P_1 in $\mathbf{Q}_{S,1}$. The leakage power caused by channel estimation transmit noise $P_{\widetilde{\mathbf{z}}_1}$ has an equivalent limiting impact on the mutual information. This capacity limiting behavior due to transmit noise was also observed and investigated for general MIMO transmissions in [6]. Similarly, the bit error ratio developed a non-zero lower bound in [5] when transmit noise was present. The upper mutual information limit utilizing the model parameters was found to be $\mathcal{I}^{\text{SAT}}(\mathbf{s}_i; \mathbf{r}_i) \approx d \log_2(1 + \gamma)$ with

$$\gamma = \frac{\sigma_{P_{ii}}^2 + \sigma_{F_{ii}}^2}{\underbrace{2 \sum_{\substack{j=1 \\ j \neq i}}^{K} \frac{P_j}{P_i} \sigma_{F_{ij}}^2}_{\text{fluctuations}} + \underbrace{M_{\text{T}} \left(\frac{1}{d} + \frac{K-1}{N_{\text{PS}}} \right) \sum_{j=1}^{K} \frac{P_j}{P_i} (\sigma_{F_{ij}}^2 + \sigma_{P_{ij}}^2) \sigma_{z_j}^2}_{\text{transmit noise}}}. \quad (21)$$

Our setup was used again in [13] to further investigate and model the effects of temporal channel change and thereby outdated precoders.

VI. Conclusion

We presented IA measurement results and proposed a model that allows to match these results in good approximation. The interference leakage power was investigated, and it was concluded that additive noise at the receiver reduces the data rate irrespective of SNR, while transmit impairments and channel variations individually introduce an upper rate limit that can not be exceeded by increasing SNR. This upper limit can be increased by improved transmit hardware or reduced precoder feedback time. A formula presented to estimate this limit utilizing the model parameters was found to be in agreement with our observations.

---

[3] We computed the mutual information between $\mathbf{x}_1$ and $\mathbf{y}_1$, i.e., without IA filters, in the interference free case and divided it by $K = 3$. Each user can exploit its full MIMO multiplexing gain of $M_{\text{T}} = N_{\text{R}} = 4$ but has only $\frac{1}{3}$ of the time to transmit data.
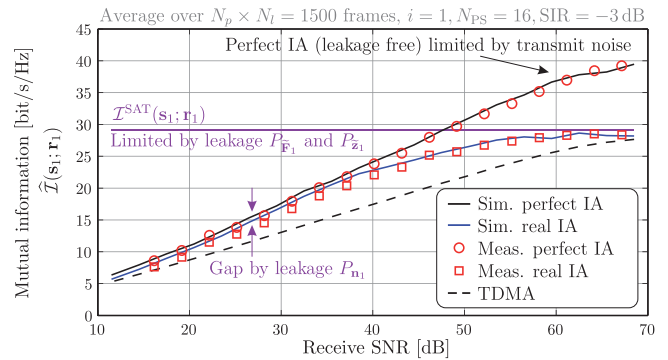
References

[1] V. R. Cadambe and S. A. Jafar, "Interference Alignment and Degrees of Freedom of the K-User Interference Channel," *IEEE Transactions on Information Theory*, vol. 54, no. 8, pp. 2435–3441, 2008.

[2] M. Razaviyayn, G. Lyubeznik, and Z.-Q. Luo, "On the Degrees of Freedom Achievable Through Interference Alignment in a MIMO Interference Channel," *IEEE Transactions on Signal Processing*, vol. 60, no. 2, pp. 812–821, 2012.

[3] O. El Ayach, S. W. Peters, and R. W. Heath, "The Feasibility of Interference Alignment Over Measured MIMO-OFDM Channels," *IEEE Transactions on Vehicular Technology*, vol. 59, no. 9, pp. 4309–4321, 2010.

[4] C. Studer, M. Wenk, and A. Burg, "MIMO transmission with residual transmit-RF impairments," in *International ITG Workshop on Smart Antennas (WSA 2010)*, pp. 189–196, IEEE, 2010.

[5] J. P. González-Coma, P. M. Castro, and L. Castedo, "Transmit impairments influence on the performance of MIMO receivers and precoders," in *11th European Wireless Conference 2011 - Sustainable Wireless Technologies (European Wireless)*, VDE, 2011.

[6] E. Bjornson, P. Zetterberg, M. Bengtsson, and B. Ottersten, "Capacity limits and multiplexing gains of MIMO channels with transceiver impairments," *IEEE Communications Letters*, vol. 17, no. 1, pp. 91–94, 2013.

[7] R. Tresch and M. Guillaud, "Cellular Interference Alignment with Imperfect Channel Knowledge," in *IEEE International Conference on Communications Workshops (ICC Workshops)*, IEEE, 2009.

[8] P. Zetterberg and N. N. Moghadam, "An Experimental Investigation of SIMO, MIMO, Interference-Alignment (IA) and Coordinated Multi-Point (CoMP)," in *19th International Conference on Systems, Signals and Image Processing (IWSSIP 2012)*, pp. 211–216, IEEE, 2012.

[9] O. El Ayach, K. Rosenfeld, R. W. Heath, *et al.*, "The practical challenges of interference alignment," *IEEE Wireless Communications*, vol. 20, no. 1, pp. 35–42, 2013.

[10] M. Mayer, G. Artner, G. Hannak, M. Lerch, and M. Guillaud, "Measurement Based Evaluation of Interference Alignment on the Vienna MIMO Testbed," *The Tenth International Symposium on Wireless Communication Systems (ISWCS), Ilmenau, Germany*, 2013.

[11] J. Balakrishnan, M. Rupp, and H. Viswanathan, "Optimal Channel Training for Multiple Antenna Systems," *Multiaccess, mobility and teletraffic for wireless communications*, vol. 5, p. 25, 2000.

[12] E. Telatar, "Capacity of Multi-antenna Gaussian Channels," *European Transactions on Telecommunications*, vol. 10, no. 6, pp. 585–595, 1999.

[13] G. Artner, M. Mayer, M. Guillaud, and M. Rupp, "Measuring the Impact of Outdated Channel State Information in Interference Alignment Techniques," *The Eighth IEEE Sensor Array and Multichannel Signal Processing Workshop (SAM 2014)*, June 2014.